

# Binocular open-view instrument to measure aberrations and pupillary dynamics

Emmanuel Chirre, Pedro M. Prieto,\* and Pablo Artal

Laboratorio de Óptica, Instituto Universitario de Investigación en Óptica y Nanofísica, Universidad de Murcia, Campus de Espinardo, E-30100 Murcia, Spain

\*Corresponding author: pegrigo@um.es

Received June 18, 2014; revised July 4, 2014; accepted July 8, 2014;  
posted July 9, 2014 (Doc. ID 214356); published August 7, 2014

We have designed and built a binocular Hartmann–Shack wave-front sensor using a single microlens array and camera for real-time aberration measurement of both eyes in an open-view configuration. Furthermore, the use of a long wavelength (1050 nm) laser diode makes the illumination source completely invisible, so that measurements can be unobtrusively performed while the subject stares at the visual world under realistic conditions. The setup provides a large dynamic range and simultaneous measurements of convergence, pupil size, accommodation, and aberrations. The open-view design not only offers the possibility of measuring the subject's ocular optics under natural conditions but also allows coupling the device with other existing vision testing instruments and setups, which increases its potential to become a powerful tool for different visual optics studies. © 2014 Optical Society of America

OCIS codes: (120.0120) Instrumentation, measurement, and metrology; (330.5370) Physiological optics; (330.7322) Visual optics, accommodation; (330.7327) Visual optics, ophthalmic instrumentation.

<http://dx.doi.org/10.1364/OL.39.004773>

Since the first implementations of the Hartmann–Shack (HS) sensor for ocular wavefront measurement by the end of last century [1–3], this technology has become widely used in clinical practice. Through the years, HS sensors have been used for a wide range of applications, such as studying the statistics of the aberrations in the human eye [4–6], analyzing their dynamics [7,8], or investigating the effects of accommodation on ocular optics [9–11]. However, most of these studies have been performed under monocular conditions, since only a very limited number of binocular HS setups have been reported [12–15].

Some of the existing binocular sensors are, in fact, a component in their respective binocular vision simulators [14,15]. As a consequence, the line of sight is fixed in order to allow wavefront manipulation, and the viewing conditions are not entirely natural. To the best of our knowledge, only two instruments have been presented working in open-view [12,13], in the sense that the subject sees the stimuli in a direct line of sight. However, one of them consists of two separate HS sensors, one for each eye [12], while the other apparently has a fixed target and does not allow the subject to fixate to different vergences [13]. Furthermore, all previous systems had the drawback of using infrared wavelengths shorter than 850 nm, which means the illumination beam has to be switched off or produces a faint red spot superimposed on the stimulus.

In this context, we present here an open-view binocular HS sensor using an invisible illumination wavelength of 1050 nm. A large dichroic mirror (see Fig. 1, top) redirects the retinal reflection to a lower plane containing the sensor while the subject can fixate to different objects or stimuli in direct vision. This feature, combined with the use of a longer wavelength at a power level that is invisible for the human eye, allows us to unobtrusively measure both eyes' aberrations while the subject performs any visual task under realistic conditions.

The HS sensor is composed of a 150- $\mu\text{m}$  pitch, 5.2-mm focal length microlens array (MLA 150-5C, Thorlabs GmbH, Germany) and a NIR CCD camera operating at 25 Hz (Hamamatsu C7500-51, Hamamatsu K. K., Japan).

The microlens array was mounted on a micrometer stage and displaced to produce the sharpest spot image when illuminated with a collimated beam. A broadband source with peak emission at 1050 nm (Broadband ASE source, 1  $\mu\text{m}$  band, Multiwave Photonics, Portugal) was used for illumination. The wavelength of this source has the advantage of being completely invisible, at least for the power levels used in our system, which are at least one order of magnitude below the safety level [16]. It has

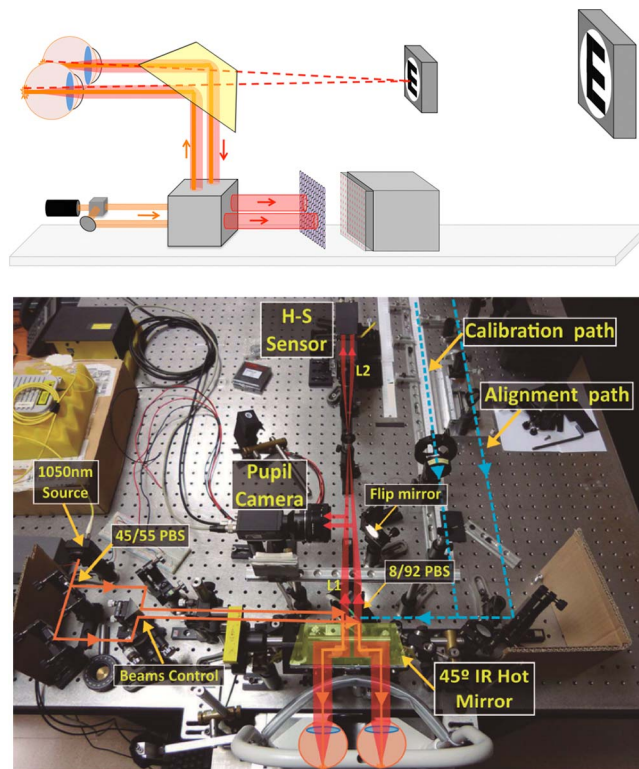


Fig. 1. Apparatus. Top: schematic view to illustrate the two level design with the H-S (HS) sensor in a lower plane with respect to the line of sight. Bottom: general view of the setup with the main components and light paths labeled.

the drawback of shifting the defocus due to the longitudinal chromatic aberration with respect to the center of the visible spectrum, but this effect was calibrated in an earlier study [17] and can easily be removed from the results. Two 1-mm diameter beams of similar intensity were produced using a single diaphragm and a 45/55 pellicle beam splitter. Both of them were reflected on an 8/92 beam splitter and directed upward, by means of two periscopes with adjustable mirrors, to separately control the position and direction of each illumination beam. A large hot mirror, tilted  $45^\circ$  from horizontal, was used to reflect the illumination beams toward the eyes and the retinal reflections toward the lower level where the HS sensor is located, while the subject has an unimpeded open view of the world in front. The reflected beams travel backward through the twin periscopes and then through a 0.5-magnification telescope in order to fit both pupils into the area of the CCD. To ensure the proper conjugation of the eyes' pupils with the HS plane, i.e., the correct positioning of the subject along the axis, a pupil monitoring camera can be reached by means of a flip mirror in front of the HS sensor. The operator's task is to move the chin rest until the subject's pupils are in focus. A couple of 900-nm LEDs, switched on only for this task, provide the convenient ambient light.

A modified software package was developed based on our binocular HS processing software [3,14]. The main new feature is a module for real-time evaluation of the pupil's position and size, from the background light in the HS images (see Fig. 2). This information is not only useful for future processing but also allows us real-time wavefront measurement with the pupil images "floating" on the CCD area. On the one hand, this reduces the requirements for fixing the subject's head, which, in our case, is performed by means of a chin rest. On the other hand, and more importantly, it enables the subject to change fixation across the field of view and not be restricted to a specific axis.

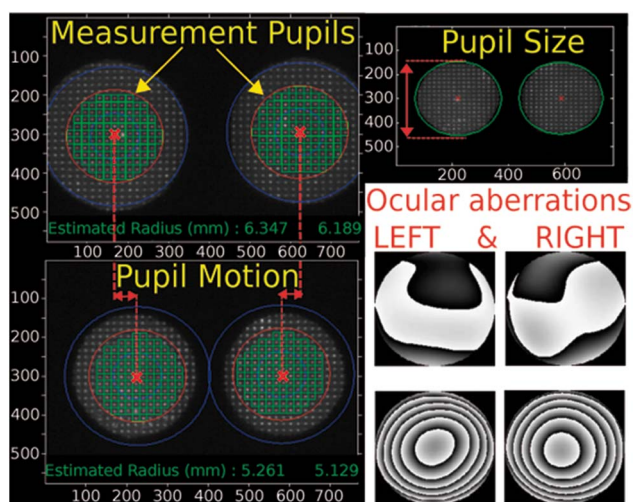


Fig. 2. Binocular measurement with on-image pupil detection. The software package processes the binocular HS image by detecting both pupil positions and calculating the associated wavefront for a specified pupil diameter around the actual pupil center. Convergence changes can be estimated from the interpupillary distance.

In order to test the accuracy and sensitivity of the system, a calibration arm was included (blue line in Fig. 1, bottom) in which known power lenses can be introduced at known distances from the HS sensor in the path of a collimated 1050-nm beam. The system linearity was checked by displacing a 10-D convergent lens along the calibration arm. This had the effect of producing a pseudo-point object at controlled distances from the microlens array and, as a consequence, known amounts of defocus. A nearly perfect linear fitting between the measured defocus and the inverse of the lens position was obtained, confirming the linearity of the system. The slope was not 1 because the actual distance between the microlens array and the CCD that produces the sharpest spot image does not coincide with the microlens nominal focal length [18]. Using a distance between elements other than the focal length does not alter the HS functioning, but scales the spot displacements. Therefore, in order to produce correct aberration coefficient values, the correct distance has to be used in the reconstruction algorithm. Additionally, since the expanding beam from the 10-D lens fills the entire HS area, the procedure was repeated using 4 small pupils close to each corner of the CCD. The computed distance was virtually the same for all 4 corners, indicating a good parallelism between the microlens array and CCD.

To test the system sensitivity, a 0.5D divergent lens was displaced in 10 cm steps. Over a 2-mm diameter pupil, this corresponds to changes in the coefficient of defocus,  $C(2,0)$ , on the order of  $0.005 \mu\text{m}$ . The measured coefficient was in good agreement with the theoretical values, revealing the sensitivity of the system.

As a proof of concept we used the binocular open-view HS sensor in an experiment where the subject voluntarily accommodated between two real objects at two different distances (see Fig. 1, top panel). Subjects were instructed to switch their attention between two large E-letters ( $1.3^\circ$  angular size), one displayed in a 19-inch LED monitor and the other shown in an OLED microdisplay located at 3 m and 30 cm, respectively, in front of the subject. Switching between objects required the subject to change binocular convergence and also to slightly change the line of sight, since the monitor and the microdisplay were at different heights in order to make them both visible simultaneously for the subject. The pupil tracking algorithm was able to cope with the associated changes in pupil position so that the evolution of accommodation and high-order aberrations can be measured in real time (25 Hz) for both eyes. Additionally, from the pupil tracking data, we estimated the change in convergence and the pupil sizes.

Figure 3 shows an example of results for one subject and they are in agreement with existing literature [12,19]. Binocular convergence was quantified by the change in interpupillary distance and resulted in the fastest process, followed by accommodation. Pupil constriction is slower than the other components of the near triad for this subject. Other young subjects tested presented a similar dynamic behavior. Spherical aberration for this subject is small in both eyes but a shift to more negative values can be seen. Although the data is too noisy to clearly establish the exact time course, it appears, at least for the right eye, where the change is more evident, to

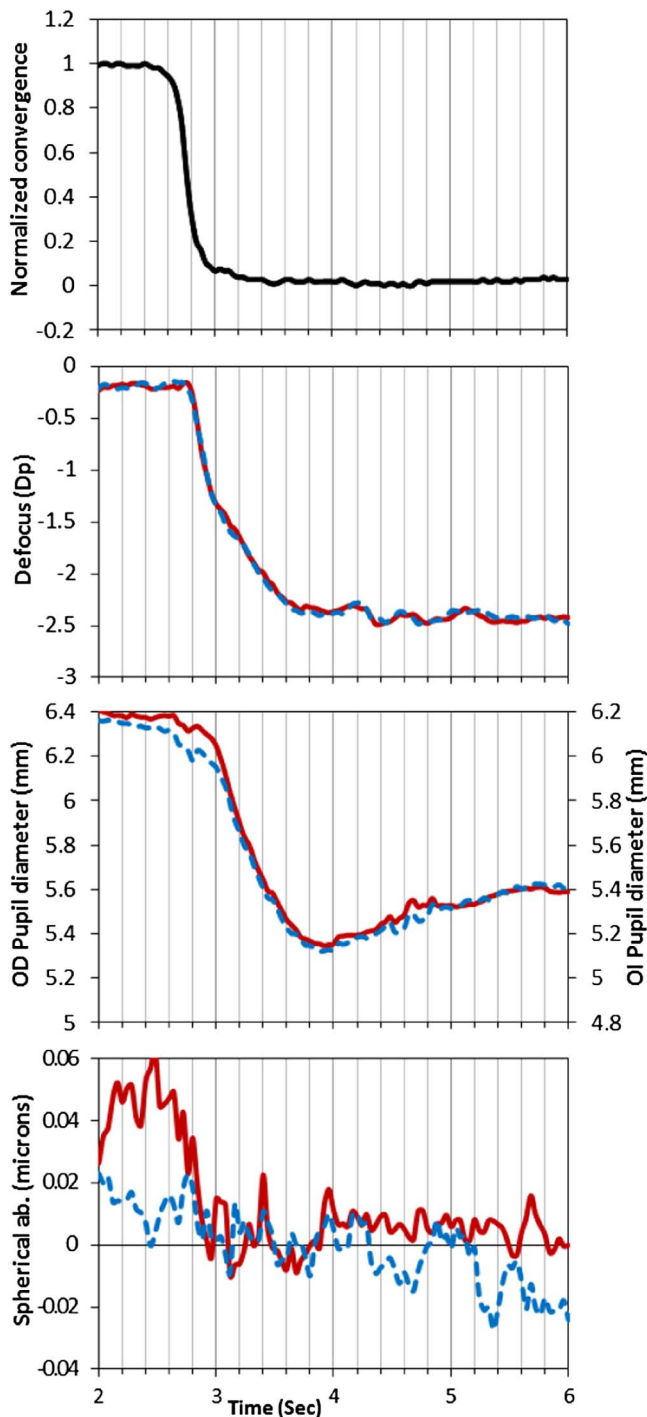


Fig. 3. Temporal behavior of the near triad and spherical aberration (for a 4-mm pupil diameter) in a subject during voluntary accommodation. Note: since the subject presented a slight anisocoria ( $\sim 0.2$  mm difference in diameter), the curves for pupil diameter are represented in a dual Y-axis scheme to highlight the similarity between time courses.

happen after convergence and may be synchronized with accommodation.

To conclude, we presented an open-view binocular HS sensor using invisible infrared illumination and capable of real-time measurements. The ability to unobtrusively measure the aberrations, accommodation, and pupil size and position in both eyes while the subject performs realistic visual tasks makes this device a powerful and versatile tool that can be used in a wide range of studies.

This research was supported by the European Research Council Advanced Grant, ERC-2013-AdG-339228 (SEECAT), to P. Artal; and by the “Ministerio de Ciencia e Innovación” (Spain) Grant n° FIS2010-14926. E. Chirre acknowledges a FPI predoctoral fellowship by the “Ministerio de Ciencia e Innovación” (Spain).

## References

1. J. Liang, B. Grimm, S. Goelz, and J. F. Bille, *J. Opt. Soc. Am. A* **11**, 1949 (1994).
2. J. Liang and D. R. Williams, *J. Opt. Soc. Am. A* **14**, 2873 (1997).
3. P. M. Prieto, F. Vargas-Martin, S. Goelz, and P. Artal, *J. Opt. Soc. Am. A* **17**, 1388 (2000).
4. J. Porter, A. Guirao, I. G. Cox, and D. R. Williams, *J. Opt. Soc. Am. A* **18**, 1793 (2001).
5. L. N. Thibos, X. Hong, A. Bradley, and X. Cheng, *J. Opt. Soc. Am. A* **19**, 2329 (2002).
6. M. P. Cagigal, V. F. Canales, J. F. Castejon-Mochon, P. M. Prieto, N. Lopez-Gil, and P. Artal, *Opt. Lett.* **27**, 37 (2002).
7. H. Hoffer, P. Artal, B. Singer, J. L. Aragon, and D. R. Williams, *J. Opt. Soc. Am. A* **18**, 497 (2001).
8. A. Mira-Agudelo, L. Lundstrom, and P. Artal, *Ophthalmic Physiol. Opt.* **29**, 256 (2009).
9. S. Ninomiya, T. Fujikado, T. Kuroda, N. Maeda, Y. Tano, T. Oshika, Y. Hirohara, and T. Mihashi, *Am. J. Ophthalmol.* **134**, 924 (2002).
10. H. Cheng, J. K. Barnett, A. S. Vilupuru, J. D. Marsack, S. Kasthurirangan, R. A. Applegate, and A. Roorda, *J. Vision* **4**(4), 3, 272 (2004).
11. S. Plainis, H. S. Ginis, and A. Pallikaris, *J. Vision* **5**(5), 7, 466 (2005).
12. M. Kobayashi, N. Nakazawa, T. Yamaguchi, T. Otaki, Y. Hirohara, and T. Mihashi, *Appl. Opt.* **47**, 4619 (2008).
13. S. Chin, K. Hampson, and E. Mallen, *Opt. Express* **16**, 14731 (2008).
14. E. J. Fernandez, P. M. Prieto, and A. Artal, *Opt. Lett.* **34**, 2628 (2009).
15. R. Sabesan, L. Zheleznyak, K. Ahmad, and G. Yoon, *Biomed. Opt. Express* **3**, 3176 (2012).
16. ANSI Z136.1-2007, American National Standard for Safe Use of Lasers.
17. E. J. Fernández and P. Artal, *Opt. Express*, **16**, 21199 (2008).
18. P. Ruffieux, T. Scharf, H. P. Herzig, R. Völkel, and K. J. Weible, *Opt. Express* **14**, 4687 (2006).
19. J. C. He, S. A. Burns, and S. Marcos, *Vis. Res.* **40**, 41 (2000).